Supplementary Information

Flexographic printed microwave-assisted grown zinc oxide nanostructures for sensing applications

Maria Morais,[a] Emanuel Carlos,[a,*] Ana Rovisco,[a] Tomás Calmeiro,[a] Hugo Gamboa,[b] Elvira Fortunato,[a] Rodrigo Martins[a] and Pedro Barquinha [a,*]

[a] CENIMAT|i3N, Department of Materials Science, School of Science and Technology, NOVA University Lisbon and CEMOP/UNINOVA, Caparica, Portugal

[b] LIBPhys (Laboratory for Instrumentation, Biomedical Engineering and Radiation Physics), NOVA School of Science and Technology, Campus de Caparica, 2829-516, Portugal

*e.carlos@fct.unl.pt; **pmcb@fct.unl.pt

The supplementary information contains relevant data concerning the equipments used to produce the pressure sensors and characterizations of the seed layers and zinc oxide (ZnO) nanorod samples resulting from different synthesis conditions. **Table S1** compares the production process and performance of the developed sensors with that of previously reported ZnO-based pressure sensors. The lab-scale flexographic printing equipment and stamps used to pattern the seed layers on PET-ITO substrates are presented in **Figure S1**. **Figure S2** shows the 2D atomic force microscopy (AFM) images of the seed layers with different zinc acetate dihydrate concentrations (0.25, 0.50 and 1 M). **Figure S3** exhibits non-patterned seed layers produced by depositing solutions with varying zinc acetate concentrations on PET-ITO substrates. **Table S2** lists the length, diameter and density of nanorod arrays synthesized with different conditions. Cross-sectional SEM images of a 1 M zinc-based seed layer deposited on a PET-ITO substrate and the ZnO nanorods grown from this layer are presented in **Figure S4**. The diffractograms of the seed layers with different zinc acetate dihydrate concentrations, namely 0.25, 0.50 and 1 M, are presented in **Figure S5**. The SEM images of the nanostructures produced from 1 M seed layers, annealed at 140 ºC, using growth solutions with different molar ratios of zinc nitrate hexahydrate and hexamethylenetetramine (HMTA) are shown in **Figure S6**. The response of sensors based on ZnO nanorods grown from 1 M seed layers using 25 mM zinc nitrate hexahydrate and HMTA growth solutions is presented in **Figure S7**. The sensitivity values of the sensors based on ZnO nanorods grown from seed layers composed of 1 square and 16 squares are presented in **Table S3**. **Figure S8** presents the output voltage of a patterned sensor over 5000 impact cycles.

S1. Production process and performance of ZnO-based pressure sensors reported in the literature

Table S1. Production process and performance of pressure sensors based on ZnO nanostructures reported in the literature.

ZnO morphology	Seed layer	Growth method	Substrate	Working range	Ref
2D ZnO sheets	**Dip-coating** (90 °C, 20 min) *Solution:* 0.5 mM potassium permanganate	**Hydrothermal synthesis** (24 h, 85 °C) *Growth solution:* 7.5 mM ZN, 3.75 mM HMTA, 0.10 M NH_3, 2 mM PEI, 0.5 mM KCl and 7.5 mM MEA	PET-ITO (60 Ω/sq) *Top electrode:* PET-ITO A = (50 × 15) mm^2	GF ~ 160 (curvatures between 30 and 90º)	1
2D ZnO nanosheets	**Dip-coating** (100 ºC, 10 min) *Solution:* 0.9 mM ZAc, 30 mM NaOH (methanol)	**Hydrothermal synthesis** (8 h, 80 ºC) *Growth solution:* 0.02 M ZN and HMTA	Anodic aluminum oxide *Top electrode:* Gold A = 1 cm^2	S = 0.0318 V/kPa 29.4 N → 5.9 V	2
ZnO nanowires	-	**Chemical vapor deposition** (900 ºC, 1h) *Precursors:* Graphite and ZnO powder	PET-ITO (60 Ω/sq) *Top electrode:* Gold	S = 0.18 V/kPa 45 kPa to 61 kPa → 1.5V to 7.5V	3
ZnO film	-	**RF sputtering**	PET-ITO electrode A = 1 cm^2	P = 10 kPa → 37.50 V	4
ZnO-PTFE composites	-	**Co-sputtering**	PET-ITO electrode A = 1 cm^2	S_1 = 75.2 V/kPa (0.01–1 kPa) S_2=12.53 V/kPa (1-10 kPa) P = 10 kPa → 121.3 V	4
ZnO nanowires	-	**Electrodeposition** (80 °C, 400 rpm, −1.0 V, 2 h) *Growth solution:* 1 M sodium nitrate + 1 mM ZN (water) *Counter electrode:* Platinum-coated titanium plate	Au (50 nm)/Ti (5 nm) on nanoimprinted PMMA substrate *Top electrode:* Au (50 nm)/Ti (5 nm) A = 0.75 cm^2	Strain = 0.015 → 1.03 V	5

		Reference electrode: Silver/silver chloride saturated with KCl			
ZnO nanowires	-	**Hydrothermal synthesis** (4 h, 85 ºC) *Growth solution:* 40 mM zinc nitride and HMTA	Ni/Au (10 nm/25 nm) in p-GaN film *Top electrode:* ITO	Tensile strain = 0.79% → 9 V (bending)	6
ZnO nanorod arrays	Magnetron sputtering	**Hydrothermal growth** (2 h, 90 ºC) *Growth solution:* 50 mM ZN and HMTA	ITO *Top electrode:* Au A = 2.25 cm^2	S= 52.9 kPa^{-1} (0-100 kPa) ~ 22 kPa → 1.031 V	7
Dispersed ZnO nanorods	**Solvothermal synthesis** (8 h at 150 °C) *Growth solution:* 0.175 M ZAc (ethylene glycol/deionized water)	**Spray coating** (80 ºC) *Solution:* 10 mg/mL ZnO NPs (IPA)	PET-ITO *Top electrode:* Ag	37 Hz, acceleration of 14.715 m/s2 → 9.12 V	8
PVDF-ZnO vertically aligned structures	**Spin-coating** (100 ºC, 1h) *Solution:* 0.03 M ZAc (ethanol)	**Hydrothermal synthesis** (3 h, 100 ºC) *Growth solution:* 0.025 M ZN and HMTA	PET-ITO *Top electrode:* PET-ITO	12 to 14 kPa → 46.64 V	9
ZnO nanorods	**Flexographic printing** (140 ºC, 10 min) *Solution:* 1M ZAc (MEP)	**Hydrothermal synthesis** (30 min, 100 ºC) *Growth solution:* 0.050 M ZN and HMTA	PET-ITO *Top electrode:* PET-ITO A = 4 cm^2	S = (0.09 ± 0.04) V/kPa	This work
ZnO nanorods	**Flexographic printing** (140 ºC, 10 min) *Solution:* 1M ZAc (MEP)	**Hydrothermal synthesis** (30 min, 100 ºC) *Growth solution:* 0.050 M ZN and HMTA	PET-ITO *Top electrode:* PET-ITO A = (16 × 0.25) cm^2	S = (0.06 ± 0.01) V/kPa	This work

ZN: zinc nitrate hexahydrate; HMTA: hexamethylenetetramine; NH_3: Ammonia; PEI: Polyethylenimine; KCl: potassium chloride; MEA:monoethanolamine; ZAc: Zinc acetate dihydrate; MEP: 1-methoxy-2-propanol

S2. Lab-scale flexographic printing equipment and stamps used to deposit the seed layers

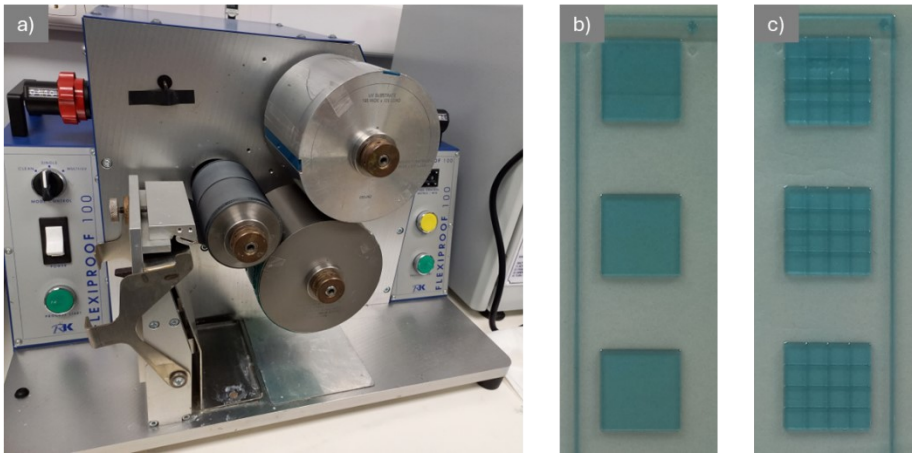

Figure S1. a) Flexographic printing equipment and (b and c) stamps used to deposit the seed layers on PET-ITO substrates. The square in b) has 4 cm^2 and the pattern in c) is composed of 16 squares of 0.25 cm^2 spaced by 0.5 μm.

S3. AFM images of the ZnO films with different zinc precursor concentrations

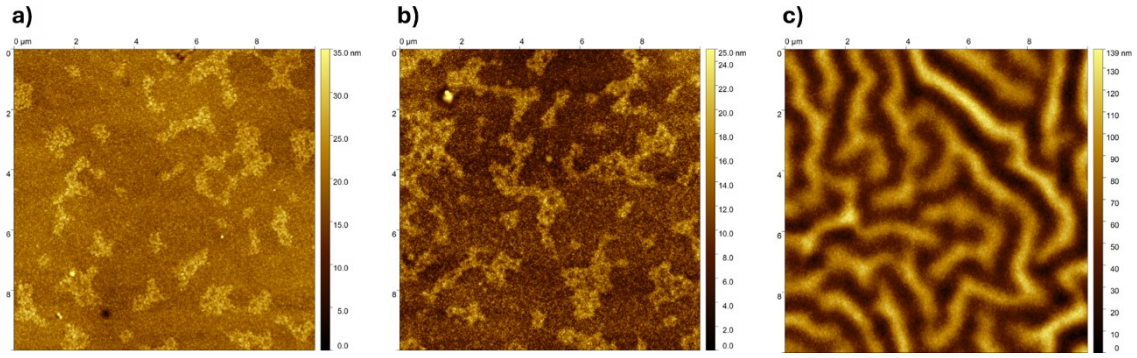

Figure S2. AFM images of the seed layers printed on PET-ITO substrates using solutions with a zinc acetate dihydrate concentration of a) 0.25, b) 0.50 and c) 1.0 M.

S4. Morphological analysis of seed layers deposited on PET-ITO substrates using solutions with different zinc precursor concentration

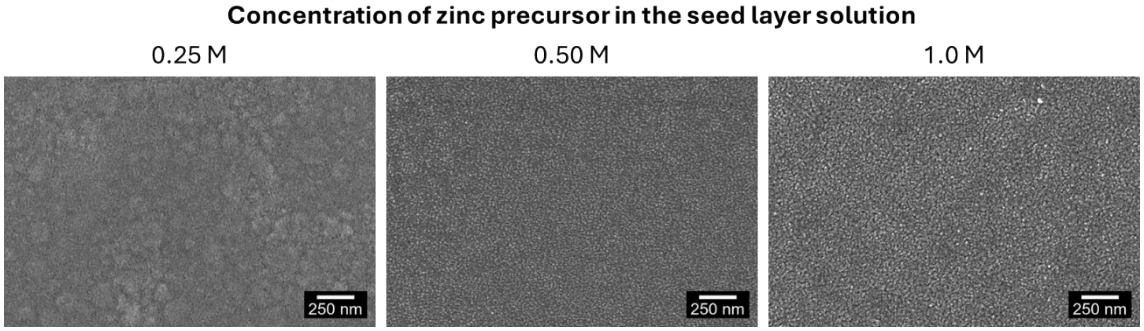

Figure S3. SEM images of the seed layers printed on PET-ITO substrates with 0.25, 0.50 and 1.0 M zinc acetate precursor solutions (non-patterned).

S5. Length, diameter and density of ZnO nanorods hydrothermally grown using different synthesis conditions

Table S2. Average values of the ZnO nanorods' length, diameter and density according to their growth conditions.

		Length (µm)	**Diameter (µm)**	**Density (nanorods/µm^2)**
Seed layer concentration	0.25 M	0.6 ± 0.1	0.18 ± 0.04	7 ± 1
	0.50 M	0.20 ± 0.04	0.0469 ± 0.005	297 ± 7
	1.0 M	0.27 ± 0.04	0.05 ± 0.01	296 ± 6
Zinc precursor	Zinc acetate	0.4 ± 0.1	0.05 ± 0.01	229 ± 2
	Zinc chloride	0.28 ± 0.04	0.046 ± 0.005	137 ± 33
	Zinc nitrate	0.27 ± 0.04	0.05 ± 0.01	296 ± 6
Precursors ratio (Zn:HMTA)	2:1	0.7 ± 0.2	0.27 ± 0.07	6 ± 1
	1:1	0.27 ± 0.04	0.05 ± 0.01	296 ± 6
	1:2	0.32 ± 0.05	0.055 ± 0.005	300 ± 25

S6. SEM-EDS analysis of 1 M zinc acetate films

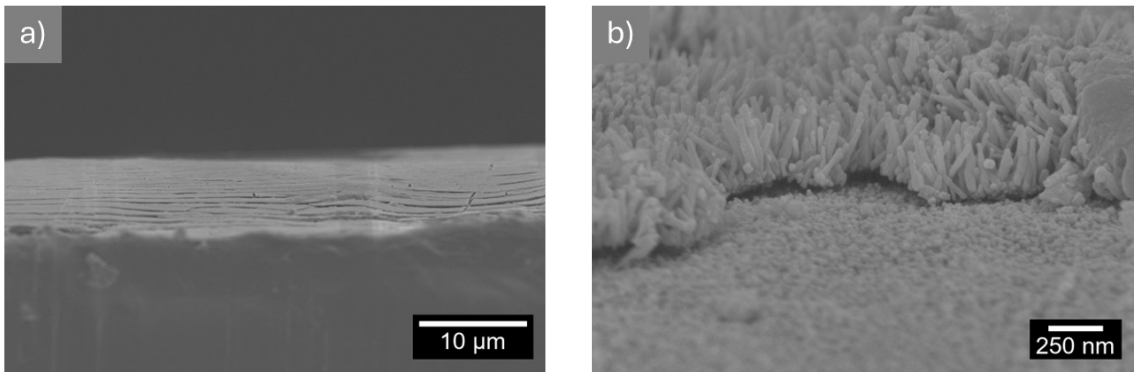

Figure S4. Cross-sectional SEM images of a) a 1 M seed layer deposited on a PET-ITO substrate and the b) ZnO nanorods grown from this layer.

S7. X-ray diffraction patterns of ZnO seed layers

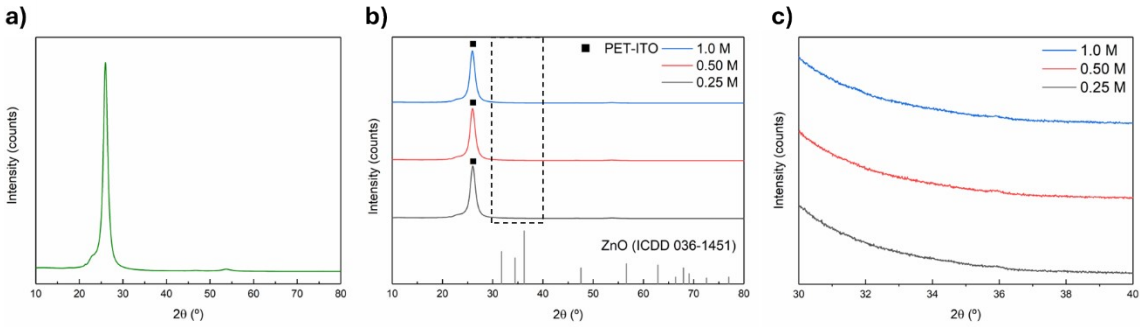

Figure S5. XRD patterns of the a) PET-ITO substrate, b) seed layers deposited on it with different zinc precursor concentrations and c) Zoom-in in the region between 30 and 40º.

S8. Morphological analysis of ZnO nanorods grown using different growth solutions

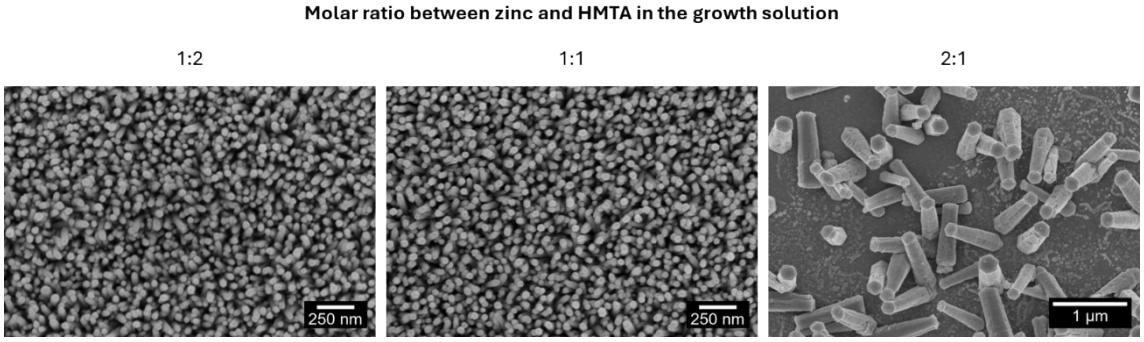

Figure S6. SEM images of ZnO nanorods grown from 1 M seed layers using growth solutions with different zinc and HMTA molar ratios.

S9. Response of pressure sensors based on ZnO nanorods grown from 25 mM zinc nitrate and HMTA solution

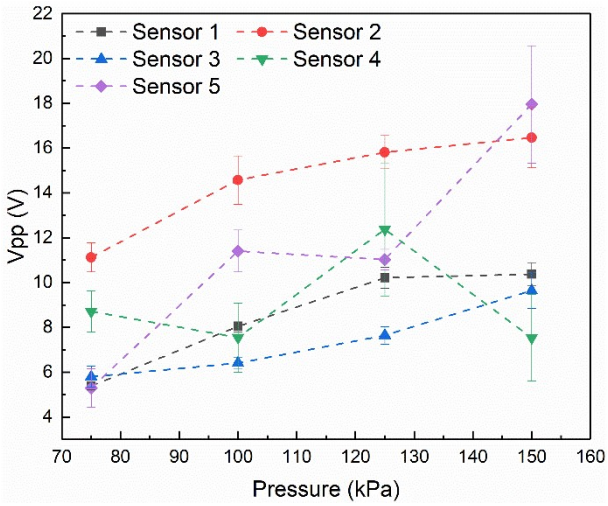

Figure S7. Peak-to-peak voltage of sensors based on nanorods grown from 1 M seed layers (single square) using 25 mM equimolar zinc nitrate hexahydrate and HMTA growth solutions.

S10. Sensitivity of the pressure sensors based ZnO nanorods with non-patterned and patterned seed layers

Table S3. Sensitivity values of the pressure sensors with 1 and 16 squares of ZnO.

Pattern		Sensitivity (V/kPa)	R^2
1 square (A = 4 cm^2)	Sensor 1	0.0891 ± 0.0009	0.99
	Sensor 2	0.06 ± 0.02	0.89
	Sensor 3	0.042 ± 0.003	0.99
	Sensor 4	0.11 ± 0.02	0.96
	Sensor 5	0.153 ± 0.001	0.99
16 squares (A = 0.25 cm^2)	Sensor 1	0.08 ± 0.01	0.96
	Sensor 2	0.038 ± 0.001	0.99
	Sensor 3	0.045 ± 0.004	0.99
	Sensor 4	0.06 ± 0.01	0.96
	Sensor 5	0.06 ± 0.01	0.96

S11. Output voltage of a patterned ZnO-based sensor over time

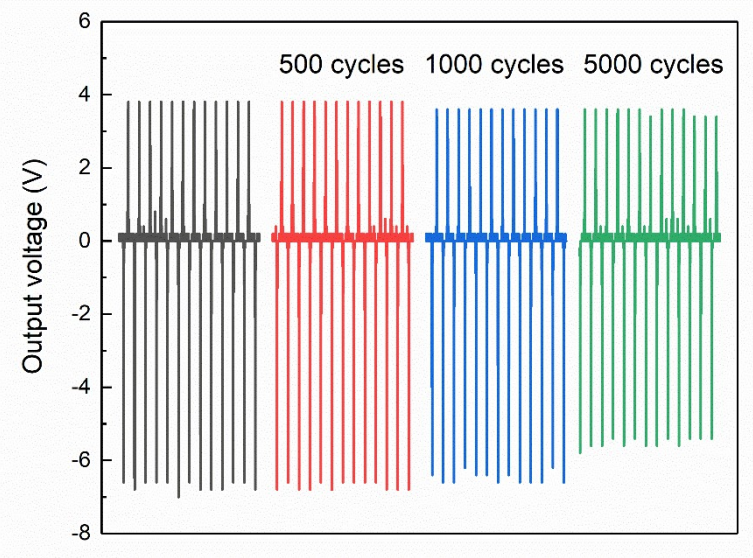

Figure S8. Output voltage of a patterned ZnO-based pressure sensor (sensor 4) for 5000 cycles.

References

1 G. Arrabito, A. Delisi, G. Giuliano, G. Prestopino, P. G. Medaglia, V. Ferrara, F. Arcidiacono, M. Scopelliti, D. F. Chillura Martino and B. Pignataro, Self-Cleaning Bending Sensors Based on Semitransparent ZnO Nanostructured Films, *ACS Appl. Eng. Mater.*, 2023, **1**, 1384–1396.

2 S. Rafique, A. K. Kasi, Aminullah, J. K. Kasi, M. Bokhari and Zafar Shakoor, Fabrication of Br doped ZnO nanosheets piezoelectric nanogenerator for pressure and position sensing applications, *Curr. Appl. Phys.*, 2021, **21**, 72–79.

3 M. Kumari, R. K. Prasad, M. K. Singh, P. K. Iyer and D. K. Singh, Piezo-resistive pressure sensor based on CVD-grown ZnO nanowires on Polyethylene Tetrathalate substrate, *arXiv (Cornell Univ.*

4 S. Ippili, V. Jella, J. M. Lee, J.-S. Jung, D.-H. Lee, T.-Y. Yang and S.-G. Yoon, ZnO–PTFE-based antimicrobial, anti-reflective display coatings and high-sensitivity touch sensors, *J. Mater. Chem. A*, 2022, **10**, 22067–22079.

5 H. Eom, J. Hur, S.-K. Sung, J.-H. Jeong and I. Park, Density-controlled electrochemical synthesis of ZnO nanowire arrays using nanotextured cathode, *Nanotechnology*, 2024, **35**, 185301.

6 Y. Peng, M. Que, H. E. Lee, R. Bao, X. Wang, J. Lu, Z. Yuan, X. Li, J. Tao, J. Sun, J. Zhai, K. J. Lee and C. Pan, Achieving high-resolution pressure mapping via flexible GaN/ ZnO nanowire LEDs array by piezo-phototronic effect, *Nano Energy*, 2019, **58**, 633–640.

7 F. Wang, J. Jiang, Q. Liu, Y. Zhang, J. Wang, S. Wang, L. Han, H. Liu and Y. Sang, Piezopotential gated two-dimensional InSe field-effect transistor for designing a pressure sensor based on piezotronic effect, *Nano Energy*, 2020, **70**, 104457.

8 E. A. Elvira-Hernández, J. Romero-García, A. Ledezma-Pérez, A. L. Herrera-May, E. Hernández-Hernández, L. A. Uscanga-González, V. A. Jarvio-Cordova, G. Hurtado, C. Gallardo-Vega and A. de León, Synthesis of ZnO Nanorod Film Deposited by Spraying with Application for Flexible Piezoelectric Energy Harvesting Microdevices, *Sensors*, 2020, **20**, 6759.

9 A. Anand and M. C. Bhatnagar, Role of vertically aligned and randomly placed zinc oxide (ZnO) nanorods in PVDF matrix: Used for energy harvesting, *Mater. Today Energy*, 2019, **13**, 293–301.